Reaction Mechanism of Glyoxalase I Explored by an X-ray Crystallographic Analysis of the Human Enzyme in Complex with a Transition State Analogue[†]

Alexander D. Cameron,*[,‡] Marianne Ridderström,[§] Birgit Olin,[§] Malcolm J. Kavarana,[||] Donald J. Creighton,[||] and Bengt Mannervik[§]

Department of Molecular Biology, Uppsala University, Biomedical Center, Box 590, S-751 24 Uppsala, Sweden, Department of Biochemistry, Uppsala University, Biomedical Center, Box 576, S-751 23 Uppsala, Sweden, and Department of Chemistry and Biochemistry, University of Maryland, Baltimore County, Baltimore, Maryland 21228

Received March 25, 1999; Revised Manuscript Received June 28, 1999

ABSTRACT: The structures of human glyoxalase I in complexes with *S*-(*N*-hydroxy-*N*-*p*-iodophenylcarbamoyl)glutathione (HIPC-GSH) and *S*-*p*-nitrobenzyloxycarbonylglutathione (NBC-GSH) have been determined at 2.0 and 1.72 Å resolution, respectively. HIPC-GSH is a transition state analogue mimicking the enediolate intermediate that forms along the reaction pathway of glyoxalase I. In the structure, the hydroxycarbamoyl function is directly coordinated to the active site zinc ion. In contrast, the equivalent group in the NBC-GSH complex is approximately 6 Å from the metal in a conformation that may resemble the product complex with *S*-D-lactoylglutathione. In this complex, two water molecules occupy the liganding positions at the zinc ion occupied by the hydroxycarbamoyl function in the enediolate analogue complex. Coordination of the transition state analogue to the metal enables a loop to close down over the active site, relative to its position in the product-like structure, allowing the glycine residue of the glutathione moiety to hydrogen bond with the protein. The structure of the complex with the enediolate analogue supports an "inner sphere mechanism" in which the GSH−methylglyoxal thiohemiacetal substrate is converted to product via a *cis*-enediolate intermediate. The zinc ion is envisioned to play an electrophilic role in catalysis by directly coordinating this intermediate. In addition, the carboxyl of Glu 172 is proposed to be displaced from the inner coordination sphere of the metal ion during substrate binding, thus allowing this group to facilitate proton transfer between the adjacent carbon atoms of the substrate. This proposal is supported by the observation that in the complex with the enediolate analogue the carboxyl group of Glu 172 is 3.3 Å from the metal and is in an ideal position for reprotonation of the transition state intermediate. In contrast, Glu 172 is directly coordinated to the zinc ion in the complexes with *S*-benzylglutathione and with NBC-GSH.

Glyoxalase I (EC 4.4.1.5) catalyzes the first of two enzymatic steps in the conversion of 2-oxoaldehydes to the corresponding 2-hydroxycarboxylic acids by way of the glyoxalase system, which uses glutathione as a cofactor (*1*−*3*). Physiologically, the reaction seems most relevant in the detoxication of methylglyoxal, which is continuously generated as a side product of glycolysis (*4*). The substrate of glyoxalase I is not methylglyoxal itself, but rather the thiohemiacetal formed when it reacts with glutathione. Glyoxalase I catalyzes the isomerization of this thiohemiacetal to *S*-D-lactoylglutathione, which is later hydrolyzed by glyoxalase II to D-lactic acid and glutathione. The reaction is thought to proceed via an enediolate intermediate with a base on the protein catalyzing the proton transfer between C1 and C2 (see Figure 1) (*5*−*7*). The enzyme has an absolute requirement for metal ions. The zinc ion in the human enzyme can be replaced by other bivalent metal ions to yield partially active enzyme (*8*, *9*). The metal ion has been proposed to indirectly facilitate catalysis via a metal-bound water molecule that stabilizes the enediolate intermediate and flanking transition states (*5*, *6*).

Recently, we determined the structure of human glyoxalase I, a homodimer with a molecular mass of 43 kDa, in a complex with *S*-benzylglutathione (B-GSH)[1] (*10*). The two active sites of the homodimer are located at the dimer interface and are characterized by a glutathione binding site, a zinc binding site, and a large hydrophobic pocket. Two amino acid residues from each subunit and one water molecule coordinate the zinc ion in a square pyramidal arrangement. These results confirmed previous conclusions

[†] Support was provided by a grant to Professor T. Alwyn Jones from the Göran Gustafsson Stiftelse, grants to T. Alwyn Jones and B.M. from the Swedish Natural Science Research Council, and a grant to D.J.C. from the National Institutes of Health.

* To whom correspondence should be addressed. Current address: Structural Biology Laboratory, Department of Chemistry, University of York, Heslington, York YO10 5DD, U.K. E-mail: cameron@yorvic.york.ac.uk. Telephone: +44 1904 432589. Fax: +44 1904 410519.

[‡] Department of Molecular Biology, Uppsala University, Biomedical Center.

[§] Department of Biochemistry, Uppsala University, Biomedical Center.

[||] University of Maryland, Baltimore County.

[1] Abbreviations: HIPC-GSH, *S*-(*N*-hydroxy-*N*-*p*-iodophenylcarbamoyl)glutathione; NBC-GSH, *S*-*p*-nitrobenzyloxycarbonylglutathione; B-GSH, *S*-benzylglutathione; rms, root-mean-square; NCS, noncrystallographic symmetry.

10.1021/bi990696c CCC: $18.00
Published on Web 09/23/1999

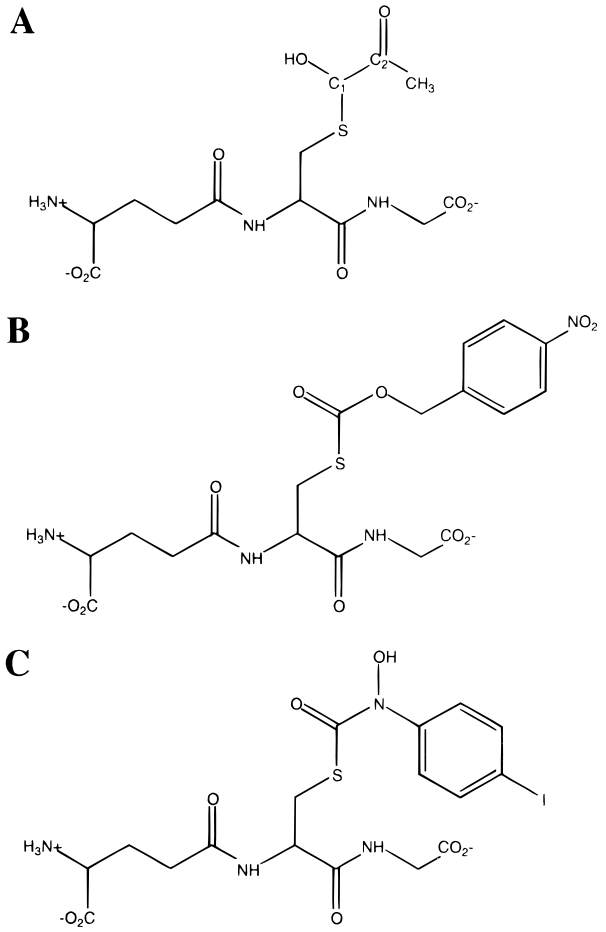

FIGURE 1: Schematic diagrams of (A) the thiohemiacetal substrate formed between glutathione and methylglyoxal, (B) *S*-*p*-nitrobenzyloxycarbonylglutathione, and (C) *S*-(*N*-hydroxy-*N*-*p*-iodophenylcarbamoyl)glutathione.

about the nature of the active site deduced from inhibitor binding and spectroscopic studies. From the structure, however, it was not obvious which residue could act as the catalytic base in the proton-transfer reaction, since the only reasonable candidates were zinc ligands. However, site-directed mutagenesis, in conjunction with the X-ray crystal structure, indicated that Glu 172, one of the zinc ligands, is critical for catalysis and is possibly the catalytic base (*11*).

Glyoxalase I has been suggested as a possible target for novel antitumor and antiprotozoal drugs, where inhibition of the enzyme would cause the buildup of cytotoxic methylglyoxal (*12*). In this regard, a number of inhibitors have been designed. The tightest binding are the *S*-(*N*-aryl-*N*-hydroxycarbamoyl)glutathione derivatives which are thought to mimic the enediolate intermediate that forms along the reaction pathway of the enzyme (*13*). A less effective inhibitor of the enzyme is *S*-*p*-nitrobenzyloxycarbonylglutathione (NBC-GSH), a compound that is structurally similar to the product of the glyoxalase I reaction (*14*).

We report here the X-ray crystal structures of human glyoxalase I in complexes with *S*-(*N*-hydroxy-*N*-*p*-iodophenylcarbamoyl)glutathione (HIPC-GSH) and with NBC-GSH (Figure 1). This comparison provides important new insights into the modes of binding of these compounds to the enzyme, and supports a reaction mechanism in which the active site zinc ion plays an electrophilic role in catalysis by directly coordinating an enediolate reaction intermediate.

Table 1: Data Collection and Refinement Statistics

	NCB-GSH[a]	HIPC-GSH
space group	$P4_3$	$P2_1$
cell dimensions	$a = b = 67.3$ Å, $c = 167.7$ Å	$a = 52.7$ Å, $b = 54.5$ Å, $c = 78.9$ Å, $\beta = 98.2°$
resolution (Å)[b]	28−1.72 (1.75−1.72)	29−2.0 (2.11−2.0)
no. of measured reflections	311697	49286
no. of unique reflections	78648	28148
completeness (%)	99.9 (100)	93.6 (93.5)
$I/\sigma I$	16.4 (4.1)	8.9 (3.2)
R_{merge} (%)	4.8 (29.1)	8.3 (19.4)
resolution range (Å)	27−1.72	29.3−2.0
R_{factor} (%)	17.4	18.0
R_{free} (%)	21.4	20.0
no. of protein atoms	5697	2800
no. of non-protein atoms	1058	256
rmsd from ideal values[c]		
bonds (Å)	0.010	0.007
angles (deg)	0.023	0.023
planes (Å)	0.024	0.023
rmsd *B* values, bonded atoms (Å^2)	1.9	1.0
no. of residues in disallowed regions of Ramachandran plot (%)[d]	0.15	0.0
average *B* value (protein) (Å^2)	18, 19, 18, 19[e]	26, 26
average *B* value (inhibitor) (Å^2)	33, 29, 32, 30[e]	21, 21

[a] A low-resolution sweep was carried out to compensate for detector overloads. [b] Values in parentheses are for the highest-resolution shells. [c] As defined by Engh and Huber (*49*). [d] Using a stringent boundary as defined by Kleywegt and Jones (*50*). [e] Values are for molecules A−D of the asymmetric unit, respectively.

MATERIALS AND METHODS

S-p-Nitrobenzyloxycarbonylglutathione Complex. The protein was expressed and purified, and native crystals were grown as described previously (*10*, *15*). A crystal was then soaked for a period of 4 days in an equivalent mother liquor containing 10 mM NBC-GSH before being transferred briefly to a similar solution containing 5% ethylene glycol. The crystal was then flash-frozen under a nitrogen gas stream at 90 K. The NBC-GSH was a gift from G. Principato (Universita' di Ancona, Ancona, Italy). Data were collected on beamline X11 at DESY (Hamburg, Germany) on a MAR Research image plate detector and integrated and merged using the HKL suite of programs (*16*). Further processing was carried out using programs from the CCP4 package (*17*). Data collection statistics are presented in Table 1.

As the starting model for refinement, the structure of the protein that had been determined in a complex with B-GSH (*10*) was used after removal of the B-GSH and all water molecules. The reflections set aside for use in the calculation of R_{free} (*18*) were equivalent to those used during the refinement of the B-GSH complex. Rigid-body refinement in X-PLOR (*19*, *20*) resulted in lowering the initial R_{factor} and R_{free} values of 45.1 and 47.1%, respectively (10−3.0 Å), to 32.7 and 32.8%, respectively. Further refinement in X-PLOR was carried out using the slow cool procedure (*21*) using all data between 7.5 and 1.75 Å and maintaining strict noncrystallographic symmetry (NCS) constraints between the four molecules of the asymmetric unit. No geometrical restraints were applied to the zinc coordination. Rebuilding of the model and inclusion of water molecules were carried out in O (*22*), using $2F_o - F_c$ maps averaged with RAVE (*23*). The glutathione moiety of the NBC-GSH was included

at this time. Since the two dimers are situated in similar crystallographic environments (the symmetry operation to move one dimer onto the other involves a 2-fold rotation around the [110] axis and translations of $^1/_2$ and $^1/_4$ along **a** and **b**, respectively), further refinement cycles were carried out with NCS constraints or restraints only between the two dimers and not between the monomers of each dimer. This was first done in X-PLOR with strict NCS constraints between the two dimers and then in REFMAC (*24*) using all data between 28 and 1.72 Å with these constraints replaced by restraints. During the final cycle, no NCS restraints were applied between molecules. The final coordinates and the structure factors have been deposited in the Protein Data Bank and assigned entry code 1QIP.

S-(N-Hydroxy-N-p-iodophenylcarbamoyl)glutathione. The expression, purification, and crystallization protocols were based on those described previously (*10*, *15*). However, the protein was eluted from the *S*-hexylglutathione affinity column with HIPC-GSH rather than with *S*-hexylglutathione, and 2.5 mM HIPC-GSH was added to the protein solution prior to crystallization. The HIPC-GSH was prepared by a method analogous to those described previously (*13*). Hexane-1,6-diol (3%) was also added to the protein mixture. Though the HIPC-GSH complex crystals were grown under conditions similar to those of the native crystals and had a similar appearance, indexing of the diffraction images showed that they belonged to space group $P2_1$ rather than $P4_3$. Data were recorded at 10 °C on an Raxis-II imaging plate detector mounted on a rotating anode generator and integrated using MOSFLM (*25*). Scaling and further processing was carried out using programs from the CCP4 suite (*17*).

The program AMoRe (*26*) was used to determine the orientation and position of the protein chain of one dimer of the NBC-GSH complex in the unit cell. Following optimization of the position in AMoRe, the model had an R_{factor} of 33.7% and a correlation coefficient of 72.2 (10−2.5 Å). Initial refinement was carried out in CNS (*27*) using the slow cool procedure and torsional angle refinement (*28*) with NCS constraints imposed. All data between 28 and 2.0 Å were used during refinement with a correction for the bulk solvent, and 5% of the reflections were set aside for use in the calculation of R_{free}. Rebuilding, including the insertion of the HIPC-GSH, was carried out in O (*22*), using $2F_o - F_c$ maps averaged with RAVE (*23*). Further refinement was carried out in REFMAC (*24*) with tight NCS restraints, and the structure was rebuilt into unaveraged maps. Water molecules were located with ARP (*29*). Again no restraints were put on the geometry of the metal coordination, and the van der Waals radius of the zinc ion was set to 0.1 Å. The final coordinates and the structure factors have been deposited in the Protein Data Bank and assigned entry code 1QIN.

RESULTS

Complex with S-p-Nitrobenzoxycarbonylglutathione

Overall Structure. The refined structure has an R_{factor} of 17.4% (27−1.72 Å), a corresponding R_{free} of 21.4%, and reasonable stereochemistry (Table 1). This model contains two protein dimers, four zinc ions, four molecules of NBC-GSH, four molecules of 2-mercaptoethanol covalently linked to each protein monomer at Cys 60, and 906 water molecules. As a consequence of the pseudosymmetry (see Materials and Methods), the two dimers are more similar to one another than the monomers of each dimer. For residues 8−180, the rms deviation in the corresponding C_α positions after superposition is 0.2 Å for one dimer compared to the other and 0.4 Å for each monomer compared to the other monomer of the same dimer. Slight differences in the main chain of the molecules occur at the N-terminus where residues 2−7 can only be seen in one molecule of each dimer, in the loops, and at the C-terminus. The three terminal residues are not well defined in any of the molecules. Overall, the structure is very similar to that of the B-GSH complex (*10*) with the rms deviation in the C_α positions calculated between this structure and each molecule of the superposed NBC-GSH complex being ∼0.3 Å. The largest differences between the structures occur at the C-terminus which, although not well-ordered in either complex, does appear to be affected by the inhibitor.

Inhibitor Binding. In each of the four molecules, the NBC-GSH is clearly defined in the associated electron density (Figure 2A). Superpositioning of the four molecules of the asymmetric unit, based on a least-squares fit of the corresponding C_α atoms, shows that the position of the NBC-GSH with respect to the protein differs only slightly among the four molecules. The rms deviation of all NBC-GSH atoms lies between 0.4 and 0.8 Å, depending on which molecules are compared. The crystal environment presumably influences this variation, since the carboxylate group of the glycine moiety of the glutathione is involved in crystal contacts in three out of four molecules. Despite these slight differences, the interactions between the glutathione moiety of the inhibitor and the protein dimer to which it is bound are very similar both to each other and to the equivalent moiety in the B-GSH complex. The similarity between the glutathione moiety in the NBC-GSH and B-GSH complexes is particularly apparent when maps averaged over the four molecules of the asymmetric unit are compared. In addition to the conservation of the interactions between the respective inhibitors and the side chains of Arg 37, Asn 103, and Arg 122, the water-mediated hydrogen bond from the amido nitrogen of the cysteine moiety of the NBC-GSH to Thr 101 $O_{\gamma 1}$ is also present in both structures (Figure 3). Another conserved water molecule is situated between the carbonyl oxygen of the cysteine moiety and the carboxylate oxygen of the γ-glutamyl moiety.

In none of the four molecules of the asymmetric unit is the S-substituent of the glutathione as well defined in the electron density as the glutathione moiety itself, perhaps reflecting incomplete substitution of the NBC-GSH in addition to some flexibility (Figure 2A). Nevertheless, it can clearly be seen that the carbonyl group of the thioester linkage is not within the inner coordination sphere of the zinc ion but instead is situated approximately 6 Å from the zinc ion with an intervening water molecule. The nitrobenzyloxycarbonyl group points down into the hydrophobic pocket and interacts with the side chains of Glu 58, Cys 60, Ile 88, and Leu 92. Although the electron density is suggestive of some flexibility of this group, the benzene ring always lies in the same plane. Cys 60 forms a mixed disulfide with 2-mercaptoethanol, which was included in the crystallization mixture. Relative to the B-GSH complex, there are no significant changes in the conformations of the side chains

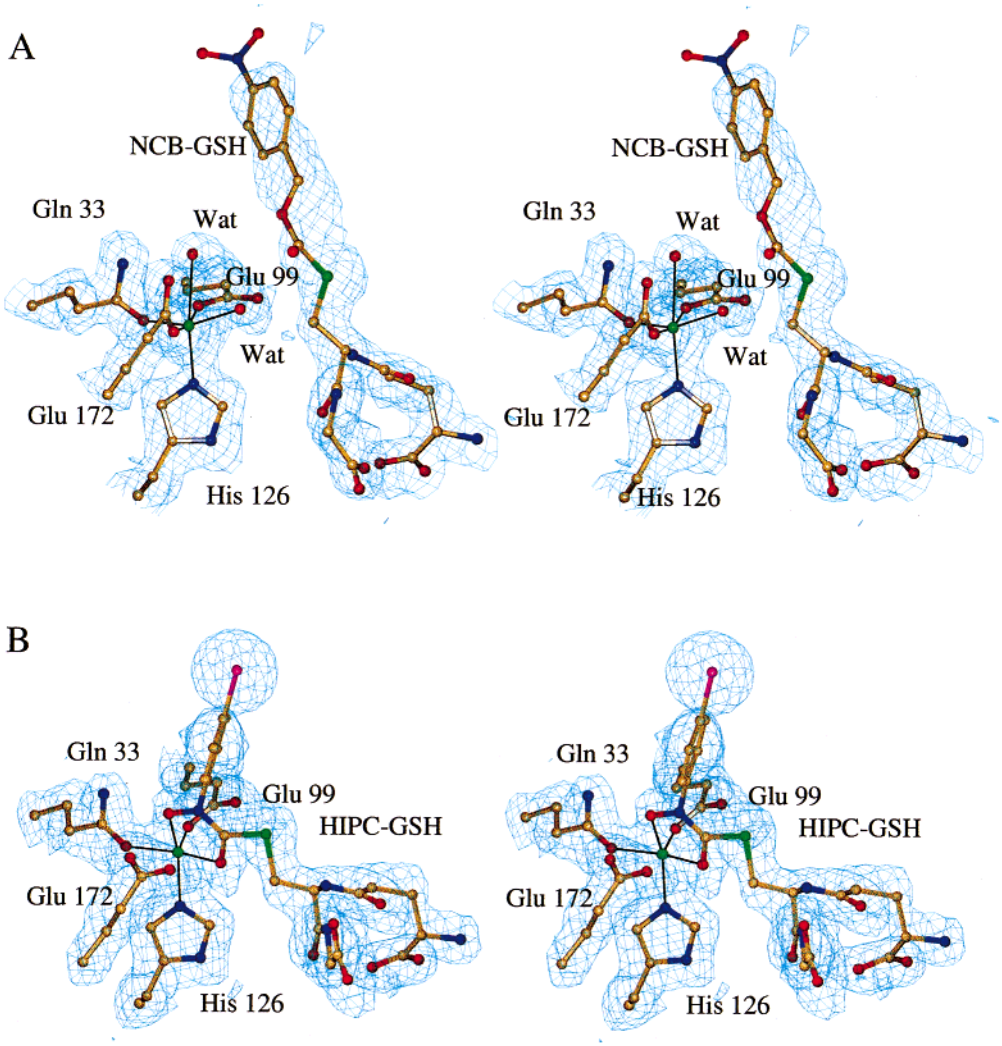

FIGURE 2: Binding of the glutathione derivatives in the vicinity of the active site zinc of human glyoxalase I. (A) Stereoview of the NBC-GSH ligand and its associated electron density. The map has been calculated using phases derived from the structure prior to the inclusion of the NBC-GSH and then subjected to 10 cycles of averaging over the four molecules of the asymmetric unit (contoured at 1σ). One of the molecules from the final structure has been superimposed. It can be seen that a water molecule is bound between the carbonyl oxygen of the glutathione and the zinc ion. (B) Stereoview of the HIPC-GSH ligand and its associated electron density. The map has been calculated using phases derived from the structure prior to the inclusion of the HIPC-GSH and then subjected to 10 cycles of averaging over the two molecules of the asymmetric unit (contoured at 1σ). One of the molecules from the final structure has been superimposed. The HIPC clearly coordinates the zinc ion.

in the hydrophobic pocket other than for Met 183, the terminal residue. If this residue were to be modeled unchanged in the B-GSH complex, it would clash with the benzene ring of the NBC-GSH. The small variations that are seen may be due to the higher resolution of the NBC-GSH data and the difference in the refinement protocols.

Zinc Coordination. The zinc ion and its respective ligands are very similar among the four molecules of the asymmetric unit. A positional deviation of ~0.1−0.2 Å was observed after superposition of the respective molecules, on the basis of a least-squares fit of the corresponding C_α atoms of residues 8−180. The distance from each of the coordinating atoms to the zinc ion is given in Table 2. There are two major differences between the geometry of coordination of the zinc ion in this complex and that seen in the complex with B-GSH (Figure 4A). In the B-GSH structure, the zinc ion has a square pyramidal coordination and is bound by the $O_{\epsilon 1}$ atoms of Gln 33, Glu 99, and Glu 172, the $N_{\epsilon 2}$ atom of His 126, and a water molecule, with His 126 as the axial ligand (*10*). In the NBC-GSH complex, there is a second water molecule on the opposite side of the zinc ion from His 126 that is ~2.6−2.9 Å from the metal (B_{factor} ~ 20−28 Å^2 as compared to 15−25 Å^2 for the first water molecule). In addition to interacting with the zinc ion, this water molecule is within hydrogen bonding distance of Gln 33 $N_{\epsilon 2}$, Glu 172 $O_{\epsilon 2}$, and the other zinc-bound water molecule (see Figure 4). Although this water molecule is a little far for coordination, the zinc ion has an approximately octahedral arrangement of ligands with an average angle of 94° between any two atoms coordinating the zinc ion.

The second difference between the two complexes is the orientation of the carboxyl functions of the glutamate residues. Relative to the B-GSH complex, Glu 99 and Glu 172 are rotated 85° and 60°, respectively, around their C_γ−C_δ bonds (see Figure 4A). The other residues are in very similar positions. In two of the four zinc sites of the asymmetric unit, single conformations of Glu 99 and Glu 172 are observed. In the other two, the electron density is

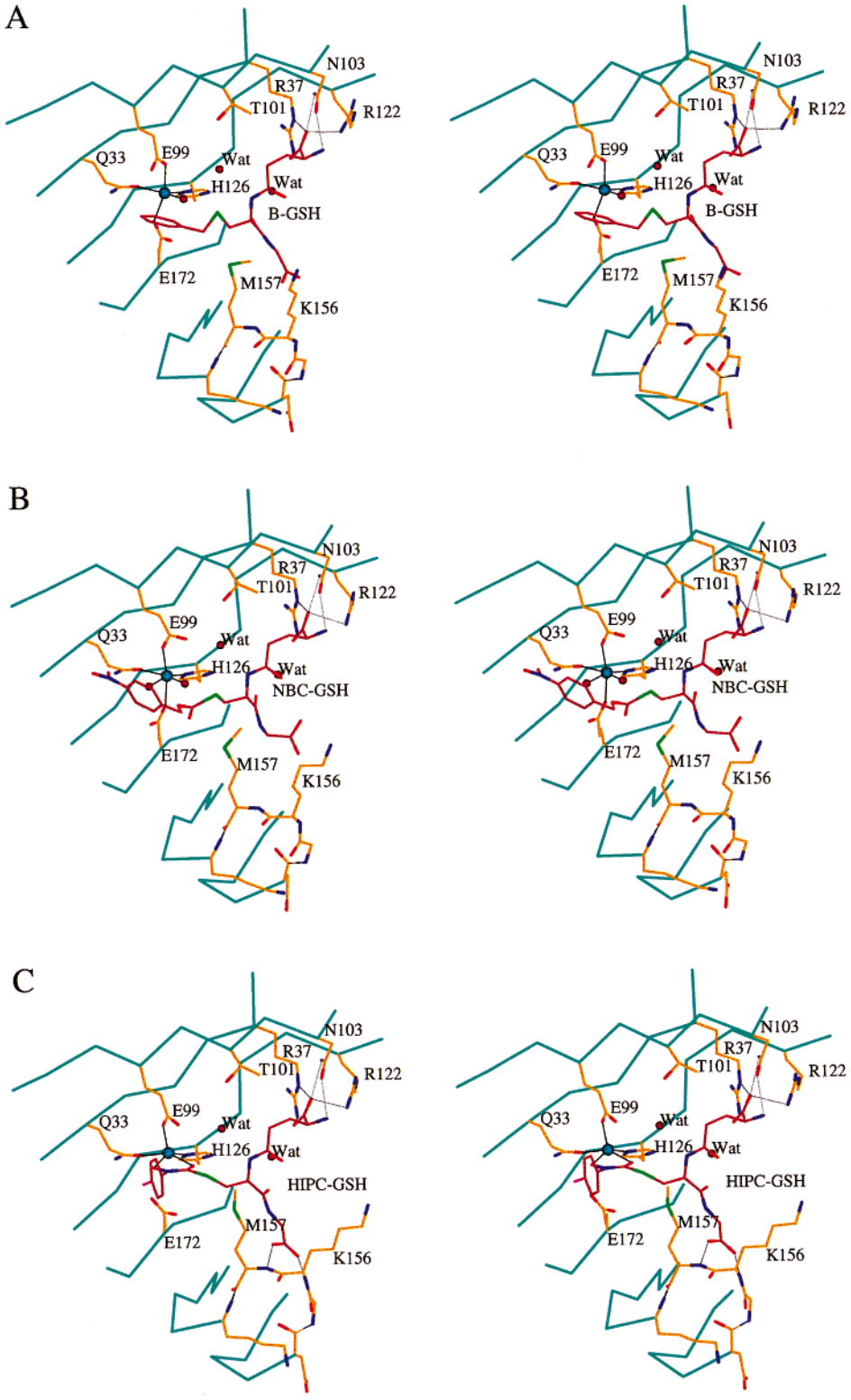

FIGURE 3: Stereoviews showing the active sites in the B-GSH (A), NBC-GSH (B), and HIPC-GSH (C) complexes. All three complexes are shown in the same view after superpositioning the respective C_α atoms. The inhibitors are shown with red-orange carbon atoms. Selected protein residues are shown with orange carbon atoms. These include the zinc ligands and the residues involved in direct or solvent-mediated hydrogen bonds with the inhibitors. The zinc is colored cyan, and water molecules are colored red. Hydrogen bonding interactions are represented by gray lines, and zinc coordination is represented by black lines.

more rounded. It is in fact possible to model a second position of Glu 99 into the electron density with the same conformation as observed in the B-GSH complex. On the other hand, the conformation seen in the NBC-GSH complex is not consistent with the electron density associated with the B-GSH structure. The difference in the orientation of the carboxylates means that the zinc ion lies within 0.2 Å of the planes of the functional groups of each of these two residues. This is much closer than those seen in the B-GSH complex [0.5 Å from Glu 99 and 1.0 Å from Glu 172 (*10*)].

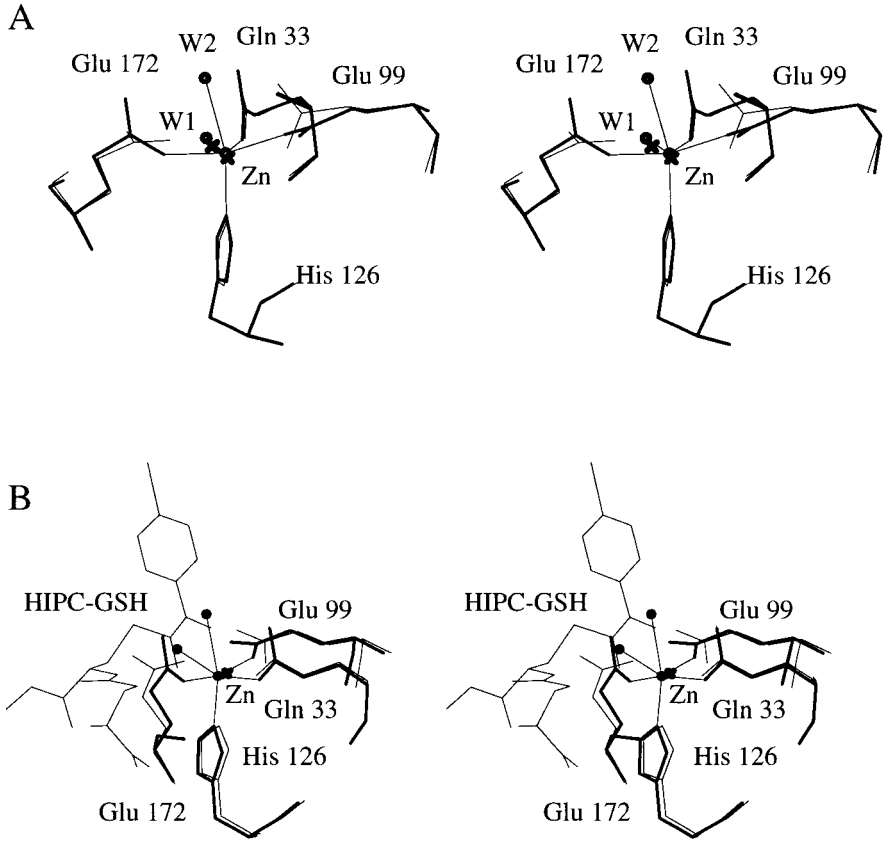

FIGURE 4: Stereoviews of the zinc coordination. (A) Comparison of the *S*-benzylglutathione complex (thin lines and ×) with the NBC-GSH complex (thick lines and ●). (B) Comparison of the NBC-GSH complex (thick lines and ●) with the HIPC-GSH complex (thin lines and ×).

Table 2: Zinc Ligand Distances (Å) in the Glyoxalase I Crystal Structures

		NCB-GSH				HIPC-GSH	
distance	B-GSH	A[a]	B	C	D	A	B
Zn−Gln 33 $O_{\epsilon 2}$	2.0	2.1	1.9	2.1	2.0	2.0	2.1
Zn−Glu 99 $O_{\epsilon 1}$	2.0	2.0	2.0	2.0	2.1	1.9	1.9
Zn−His 126 $N_{\epsilon 2}$	2.0	2.0	2.1	2.1	2.1	2.1	2.1
Zn−Glu 172 $O_{\epsilon 1}$	2.0	2.0	2.0	2.0	2.0	3.3	3.3
Zn−Wat 1/O	2.1	2.3	2.1	2.2	2.1	2.1	2.1
Zn−Wat 2/OH	−	2.6	2.8	2.9	2.8	2.1	2.0

[a] The four molecules of the asymmetric unit are denoted A−D for the NCB-GSH structure and A and B for the HIPC-GSH structure.

Complex with S-(N-Hydroxy-N-p-iodophenylcarbamoyl)-glutathione

Overall Structure. The refined structure has an R_{factor} of 18% (30−2.0 Å) and a corresponding R_{free} of 21%. The model contains one dimer of glyoxalase I (with residues from 8 to 183 of each monomer), two zinc ions, two molecules of HIPC-GSH, and a total of 192 water molecules. Due to the noncrystallographic restraints applied during refinement, the rms deviation in the positions of the corresponding C_α atoms of all residues between positions 8 and 180 after superposition of the two molecules is very low (0.04 Å). Overall, the structure is similar to those of the B-GSH and NBC-GSH complexes (rms deviation in the positions of the corresponding C_α atoms after superposition being ∼0.4−0.5 Å for all residues between positions 8 and 180). Most of the differences between this and the other structures arise from variations in the crystal environment. There is, however, a small but significant conformational change involving the loop, including residues 152−159 (Figure 5). The loop is situated between the two outermost β-strands (β7 and β8) of the barrel that forms the active site and helps to shield the substrate from the surrounding solvent. Relative to the other structures, the C_α atom of Lys 156, which is situated at the tip of the loop, has moved ∼3 Å toward the active site. This conformational change was observed to occur in both molecules of the dimer when the NBC-GSH model was subject to a cycle of refinement against the HIPC-GSH complex data using simulated annealing and without non-crystallographic symmetry restraints. Again the positions of the C-terminal residues deviate from those seen in the other structures. The electron density associated with these residues is much better defined than that seen in the other complexes.

Inhibitor Binding. In both molecules of the dimer, the HIPC-GSH is extremely well-defined in the electron density (Figure 2B). This compound has a much lower average *B* value relative to the protein than was observed for the inhibitors in either the B-GSH or the NBC-GSH complex (see Table 1). The γ-glutamyl moiety makes contacts with the protein very similar to those seen in the other structures, and even here, the two water-mediated interactions mentioned above are present (Figure 3). On the other hand, an approximately 15° change in the torsion angle around the bond between the amide nitrogen and C_α atom of the cysteine residue of the glutathione moiety, together with other smaller changes, causes a shift in the relative positions of the glycine and the S-substituent (Figures 3 and 5). This change, in conjunction with the movement of the loop between β7 and

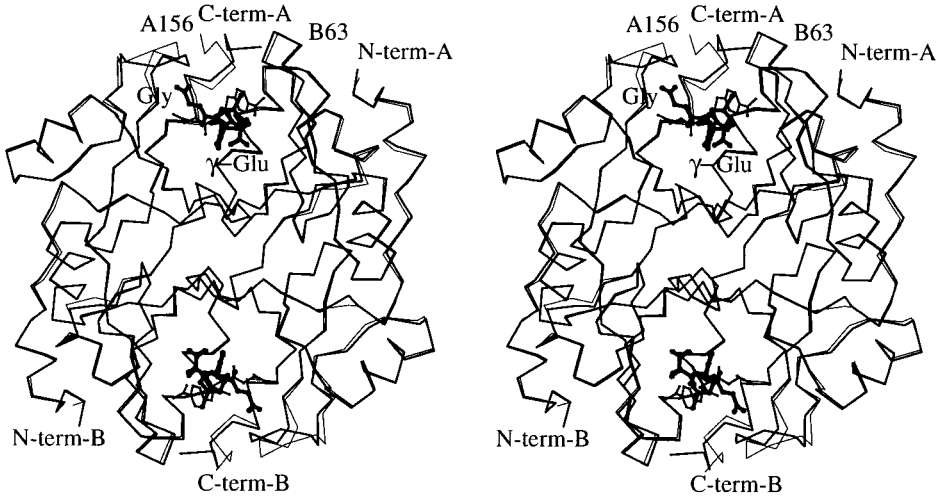

FIGURE 5: Stereodiagram showing the superposition of the NBC-GSH complex (thin lines) with the HIPC-GSH complex (thick lines) looking down the 2-fold axis of the dimer. The two inhibitors are represented by balls and sticks. The γ-glutamate and glycine moieties of the glutathione derivatives are indicated. The figure clearly shows the closure of the loop in the HIPC-GSH complex with respect to the NBC-GSH structure (residue 156 at the tip of the loop is highlighted) and the concomitant movement of the glycine moiety of the HIPC-GSH toward the loop.

β8 toward the active site, brings the carboxylate oxygens of the glycine moiety to within hydrogen bonding distance of the main chain nitrogens of Met 156 and Lys 157 (Figure 3). In the other structures, the distance between the corresponding atoms is approximately 7 Å.

For the S-substituent, the conformational change of the glutathione moiety serves to bring the hydroxycarbamoyl group toward the zinc ion so that the two oxygen atoms are within coordination distance of the metal ion. The *p*-iodophenyl group is completely shielded from the solvent with the iodine atom situated in a similar position with respect to the center of the benzene ring of bound NBC-GSH (Figure 5). Relative to the other structures, there are a number of side chains that have moved, but these are either on the flexible loop (Met 157 and Leu 160) that packs onto the inhibitor or on the C-terminal helix.

Zinc Coordination. The $O_{\epsilon 1}$ atoms of Gln 33 and Glu 99 and the $N_{\epsilon 2}$ atom of His 126 coordinate the zinc ion (see Figure 4A). However, the distance between the zinc ion and the $O_{\epsilon 1}$ atom of Glu 172 in this complex is 3.3 Å, which is too far for direct coordination. This increased separation of 1.2 Å, relative to the other structures, is caused partly by a small conformational change of the side chain of Glu 172 and partly by the movement of the two glutamic acid residues away from each other with the zinc ion following Glu 99. The two oxygen atoms of the hydroxycarbamoyl group take the place of the water molecules seen in the NBC-GSH structure, giving the metal a square pyramidal coordination. The mean angle between any two of the atoms coordinated to the zinc ion via the metal is 97°. The ligand−zinc distances are given in Table 2. The amido group of Gln 33, the hydroxycarbamoyl group of the HIPC-GSH, and the $N_{\epsilon 2}$ atom of His 126 lie in a plane with the zinc ion ~0.5 Å below this plane. The rms deviation of the atoms making up the plane from the plane is 0.05 Å. The zinc lies ~0.2 Å out of the plane of the functional group of the axial ligand, Glu 99, which adopts a conformation in which its carboxylate group is rotated by ~16° with respect to that seen in the NBC-GSH complex (see Figure 4B). Gln 33 and His 126 adopt conformations similar to those observed in the other structures.

DISCUSSION

Inhibitor Binding and Conformational Changes. Over the past three decades, many S-substituted glutathione derivatives have been tested as inhibitors of glyoxalase I. The earliest studies demonstrated that binding is a function of the hydrophobicity of the S-substituent, presumably reflecting the presence of a hydrophobic binding pocket in the active site (*30*−*32*). The strongest inhibitor of human erythrocyte glyoxalase I was *S*-*p*-bromobenzylglutathione (K_i = 0.08 μM) (*8*). More recently, *S*-(*N*-hydroxy-*N*-methylcarbamoyl)-glutathione has been proposed as a transition state analogue mimicking the enediolate intermediate that forms along the reaction pathway of the enzyme. In support of this assertion, the K_i value with yeast glyoxalase I is 30-fold lower than that of *S*-D-lactoylglutathione and 7-fold lower than the K_m of the glutathione−methylglyoxal thiohemiacetal substrate (*33*). The enediol analogue is a moderately strong competitive inhibitor of the human enzyme (K_i = 1.7 μM) (*33*). The *S*-(*N*-aryl-*N*-hydroxycarbamoyl)glutathione derivatives were subsequently discovered to be much stronger inhibitors, with K_i values that decrease with increasing hydrophobicity of the aryl substituent. The strongest inhibitor that was tested was the *p*-bromophenyl derivative (K_i = 0.014 μM) (*13*).

Fluorescence quenching experiments indicate that binding of glutathione, *S*-*p*-bromobenzylglutathione (*5*), and the *S*-(*N*-aryl-*N*-hydroxycarbamoyl)glutathione derivatives (*34*) causes a small conformational change in the enzyme. In contrast, binding of the product *S*-D-lactoylglutathione produces no change in the intrinsic fluorescence of the protein (*5*, *34*). The fluorescence quenching experiments, together with proteolytic susceptibility studies, led Creighton and coworkers to propose the presence of a flexible loop near the active site that closes over the bound enediolate analogue. They further proposed that the loop is stabilized in an open conformation in the presence of bound *S*-D-lactoylglutathione (*34*). Paramagnetic nuclear relaxation studies, using the Mn^{2+}-substituted enzyme, indicated that the carbonyl and

hydroxyl oxygens of bound *S*-D-lactoylglutathione are in the second coordination sphere of the metal, precluding direct coordination interactions (*6*, *7*).

The recently determined crystal structure of the human enzyme in complex with B-GSH confirmed some of the predictions of the inhibitor binding studies (*10*). The active site includes a large hydrophobic pocket containing the benzyl function of the bound ligand. In addition, a water molecule was observed between the sulfur atom of the ligand and the metal ion. From a single structure, no information about conformational changes could be gained. However, the specific residues that were proposed to form the flexible loop, on the basis of sequence comparisons with the "catalytic loop" of triosephosphate isomerase, belong to the β-sheet forming the core of the protein.

A comparison of the crystal structures of the binary complexes of the enzyme and the transition state analogue *S*-(*N*-hydroxy-*N*-*p*-iodophenylcarbamoyl)glutathione and product analogue *S*-*p*-nitrobenzyloxycarbonylglutathione shows that there is an intimate relationship between the nature of the S-substituent and the conformation of the bound ligand. Both ligands have bulky S-substituents, and like *S*-D-lactoylglutathione, both are thioesters of glutathione. They differ from the product at the C2 atom (Figure 1). In HIPC-GSH, an N-OH group replaces the C-OH group. In NBC-GSH, an ether oxygen replaces the C-OH of the product. The nature of this group has a dramatic influence on the mode of binding of the ligand. In the case of the HIPC-GSH−enzyme complex, the hydroxycarbamoyl group of the ligand is directly coordinated to the zinc ion. In contrast, the analogous group of NBC-GSH in a complex with the enzyme is outside the inner coordination sphere of the metal ion. This latter compound appears to bind in a manner similar to that reported for *S*-D-lactoylglutathione, on the basis of paramagnetic relaxation measurements (*6*, *7*).

Presumably, the geometry of the hydroxycarbamoyl group of HIPC-GSH allows coordination to the metal ion. This interaction has long-range effects. To coordinate the metal, the HIPC-GSH must have a conformation different from that of NBC-GSH. This brings the glycyl residue of the glutathione function near the flexible loop between β7 and β8 (residues 152−159). At the same time, this loop moves down into the active site so that the side chain of Met 157 remains within van der Waals distance of the inhibitor which has moved closer to the zinc ion. These movements enable the glycyl moiety to hydrogen bond to the main chain nitrogens of residues 156 and 157 (Figure 3). The side chain of Met 157 has been shown to play a useful role in forming the substrate binding site, since replacement of this residue with an alanine results in a significant loss of enzyme activity (*35*).

These results show that there is a flexible loop over the active site of glyoxalase I. The hydrogen bonding pattern of the loop in the open and closed conformations suggests that the loop is open in the absence of bound ligand, which enables the substrate or inhibitor to enter the active site. For the loop to close, the ligand must bind in a conformation similar to that found in the HIPC-GSH structure. The structural results are consistent with the fluorescence experiments. In addition, the structural data explain the following observations. First, the replacement of the N-OH group of *S*-(*N*-hydroxy-*N*-methylcarbamoyl)glutathione with N-H causes a significant (80-fold) decrease in binding affinity, while there is little change in affinity when the C-OH group of *S*-D-lactoylglutathione is substituted with C-H (*13*). Second, ethylation of the glycyl residue of the glutathione moiety decreases the binding affinity of the enediolate analogue, but has little affect on the binding affinity of *S*-D-lactoylglutathione (*13*). Ethylation of the glycyl residue of the glutathione also affects the binding of *S*-*p*-bromobenzylglutathione, suggesting that this compound hydrogen bonds to the closed loop (*36*). This suggestion is reinforced by the results of the fluorescence experiments, which indicate that the loop closes when *S*-*p*-bromobenzylglutathione binds to the enzyme.

Both NBC-GSH and HIPC-GSH have larger S-substituents than *S*-benzylglutathione. Nevertheless, these bulky groups are easily accommodated in the hydrophobic pocket of the protein with minimal movement of the side chains lining the pocket. Apart from the differences caused by the position of the flexible loop, only the C-terminal helix seems to vary among the three complexes. This helix appears to be fairly mobile.

Zinc Coordination. Previous EXAFS studies with human glyoxalase I (*37*) and EPR experiments with the Co^{2+}- and Cu^{2+}-substituted enzymes (*38*, *39*) indicated distorted octahedral coordination geometry for the metal ion. Interestingly, zinc ions in proteins generally have tetrahedral coordination geometries (*40*). NMR studies of glyoxalase I indicate that two of the zinc ligands are rapidly exchanging water molecules (*5*). One of these is either immobilized or displaced from the metal ion when *S*-*p*-bromobenzylglutathione or the product binds to the enzyme (*5*). In the X-ray structure of the binary B-GSH−enzyme complex, the zinc ion has a square pyramidal coordination geometry (*10*). The ligands to the Zn^{2+} include four protein residues (Gln 33, Glu 99, His 126, and Glu 172) and one water molecule. Introduction of an additional water molecule, to form an octahedral coordination field, appears to be precluded by steric interactions with the benzyl group of bound B-GSH. In the NBC-GSH complex, a water molecule does indeed interact with the zinc ion in this position, giving the metal ion an approximately octahedral coordination. The zinc to water distance is, however, larger than expected for a zinc ligand (*40*, *41*). A water molecule a similar distance from the zinc ion was also seen in the crystal structure of the double mutant Q33E/E172Q crystallized with *S*-hexyl-GSH present in the active site (*11*). In the HIPC-GSH complex, the oxygen atoms of the hydroxycarbamoyl group of the inhibitor replace the two water molecules. In addition, Glu 172 is displaced from the inner coordination sphere of the metal ion, presumably by a combination of stereochemical and electrostatic effects. Despite these differences, the zinc ion has again a square pyramidal coordination.

On the basis of the comparison of the three structures, it would seem that whereas His 126 and Glu 33 interact tightly with the metal ion in a fixed conformation, the other ligands are reasonably flexible and can move to accommodate the different inhibitors. These results are consistent with an ionic rather than a covalent nature of the interactions between the carboxylates and the zinc ions. EXAFS studies also predicted that the nature of the inhibitor might affect the orientation of two of the zinc ligands (*37*). Whereas it was inferred from the EXAFS experiment that two imidazole rings would rotate, our results show that it is the two carboxylates bound

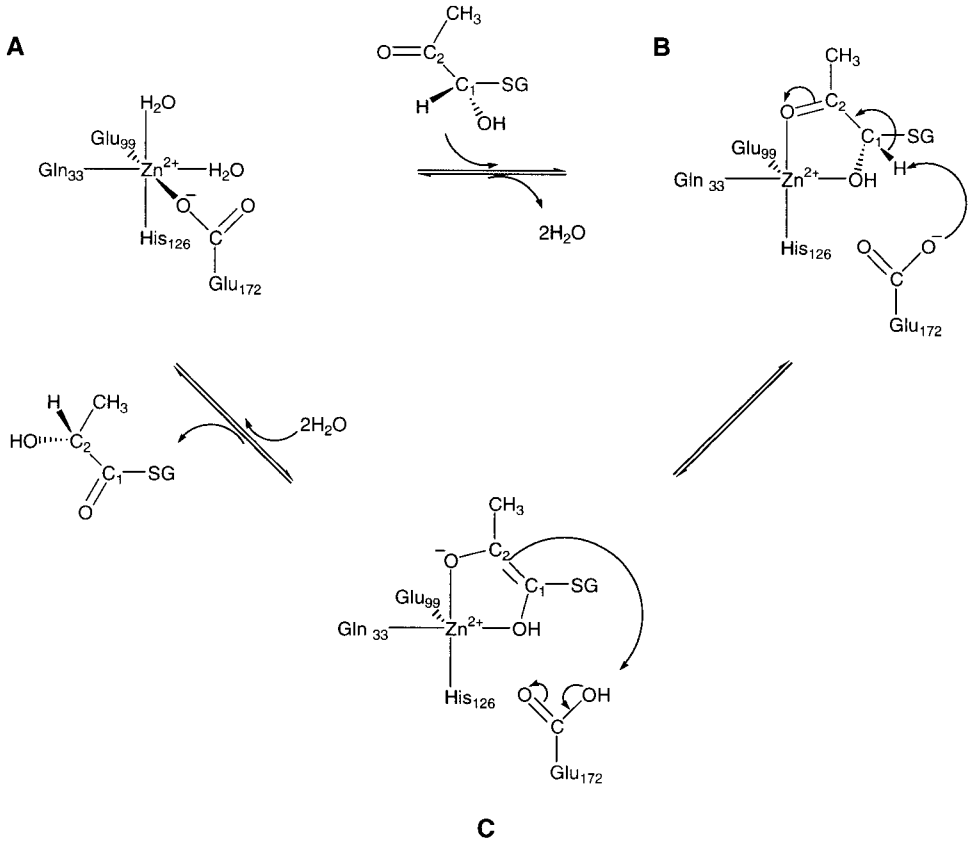

FIGURE 6: Simplified reaction mechanism for glyoxalase I (see the text).

to the zinc ion that differ in conformation between the structures. What causes the difference, however, is a matter of speculation. On the basis of the out-of-plane distances of the zinc ions from the carboxylate functional groups, it could be argued that the geometry of coordination seen in the NBC-GSH complex is the more favorable. In the B-GSH complex, the carboxylates may have altered their positions to counteract the loss of the water molecule occluded by the binding of the B-GSH.

Reaction Mechanism. An enediol proton-transfer mechanism is now generally accepted for glyoxalase I. The fact that the native enzyme depends on Zn^{2+} for activity implies that the metal ion plays an important role in catalysis. On the basis of NMR studies of the binding of the product, *S*-D-lactoylglutathione, and the apparent substrate analogue *S*-acetonylglutathione, the metal was proposed not to interact directly with the substrate or intermediate but rather to facilitate catalysis through outer sphere effects (*5*−*7*, *42*). This is consistent with a report that replacement of Zn^{2+} with V^{2+} or Ga^{3+} results in enzyme species with k_{cat} values that are larger than the ligand exchange rates of these metals in aqueous media (*3*). The structural results reported here, however, do not support such a mechanism.

In the structure of the enzyme in a complex with HIPC-GSH, the inhibitor is coordinated to the metal ion. HIPC-GSH is a tight binding competitive inhibitor of human glyoxalase I (K_i = 10 nM) that mimics the stereoelectronic features of the enediolate reaction intermediate. Its conformation in the structure strongly implies that the reaction proceeds through a metal-coordinated *cis*-enediolate intermediate. Previously, we proposed a reaction mechanism in which Glu 172, one of the zinc ligands, may act as the base in the reaction (*10*, *11*). The complex with HIPC-GSH provides further support for this mechanism since in this structure Glu 172 is not coordinated to the zinc ion as in the other complexes. Moreover, its $O_{\epsilon 2}$ carboxylate oxygen is ~3.3 Å from the C1 and N atoms of the intermediate analogue in an ideal position for the residue to act as the base.

It is well established that glyoxalase I produces D-lactoylglutathione exclusively from the racemic thiohemiacetal substrate (*43*). Pulse-chase isotope-trapping studies and NMR measurements indicate that both the *S*- and *R*-diastereomers of the substrate are used by the enzyme (*44*−*46*). Two different types of mechanisms have been proposed to account for this observation. On one hand, it has been suggested that the enzyme catalyzes the interconversion of the two bound diastereomers before only one of the diastereomers is converted to product (*44*). On the other hand, others have proposed a mechanism wherein each diastereomer is separately processed to the product via a *cis*-enediolate intermediate without prior interconversion of the different substrate forms (*47*). Modeling studies indicate that the configuration of the *S*-diastereomer of GSH−methylglyoxal thiohemiacetal is ideally suited for abstraction of the C1 proton by Glu 172 to form the *cis*-enediolate intermediate. Reprotonation of the zinc-bound intermediate by Glu 172 would result in D-lactoylglutathione. However, it is much harder to model the *R*-diastereomer so that Glu 172 would be in a position to abstract the proton to form the *cis*-enediolate. It is tempting to suggest that Glu 99, diametrically opposite Glu 172 in the zinc coordination sphere, could act as the base when the *R*-diastereomer of the substrate is present in the active site. Though this residue is coordinated

to the metal ion in all the structures, it is flexible and in the complex with HIPC-GSH its $O_{\epsilon 2}$ atom is close to the C1 and N atoms of the intermediate (3.1 and 3.2 Å, respectively). Site-directed mutatgenesis studies, though ambiguous, do indicate that the residue may play some role in the reaction mechanism (*11*). However, its position with respect to the metal-coordinated endiolate intermediate excludes it from reprotonation at C2 since this would result in L-lactoylglutathione. In the above discussion, we have not mentioned the transfer of the hydrogen that is situated on the oxygen at C1 of the substrate (Figure 1) and the oxygen at C2 of the product. With respect to the oxygens of the intermediate, both Glu 172 and Glu 99 are in suitable positions to aid in the transfer.

A simplified reaction mechanism with the *S*-diastereomer of the substrate would be as follows (Figure 6). Substrate first enters the active site and is anchored by its γ-glutamate moiety. It then swings in toward the zinc ion, displacing the metal-bound water molecules and Glu 172. This interaction presumably stabilizes the closed conformation of the peptide loop over the active site. The glycyl moiety of the substrate is important for transition state stabilization since the value of k_{cat}/K_m for the GSH−methylglyoxal hemithioacetal is 10-fold higher than the value for its glycyl ethyl ester (*48*). Glu 172 then abstracts the proton from C1, forming a *cis*-enediolate intermediate that is coordinated to the zinc ion. It should be emphasized that displacement of Glu 172 from the inner coordination sphere of Zn^{2+} during substrate binding should cause a dramatic increase in the pK_a of the carboxyl group. At the same time, direct coordination of the substrate to the metal ion should decrease the pK_a of C1-H. These shifts in pK_a are in the right direction to promote catalysis. Reprotonation at C2 results in the formation of the product, which will then dissociate from the zinc ion. This will cause the flexible loop to open and facilitate the diffusion of the product from the active site. In this mechanism, we have omitted any discussion of the transfer of the proton from the oxygen at C1 to the oxygen at C2 that must occur.

ACKNOWLEDGMENT

We are grateful to Professor T. Alwyn Jones for critical reading of the manuscript and to Professor Giovanni Principato (Universita' di Ancona) for providing the NBC-GSH ligand.

REFERENCES

1. Mannervik, B. (1980) in *Enzymatic Basis of Detoxication* (Jakoby, W. B., Ed.) Vol. 2, pp 263−273, Academic Press, New York.
2. Thornalley, P. J. (1990) *Biochem. J. 269*, 1−11.
3. Vander Jagt, D. L. (1989) in *Coenzymes and Cofactors* (Dolphin, D., Poulson, R., and Avramovic, O., Eds.) Vol. 3A, pp 597−641, John Wiley and Sons, New York.
4. Richard, J. P. (1991) *Biochemistry 30*, 4581−4585.
5. Sellin, S., Eriksson, L. E. G., and Mannervik, B. (1982) *Biochemistry 21*, 4850−4857.
6. Sellin, S., Rosevear, P. R., Mannervik, B., and Mildvan, A. S. (1982) *J. Biol. Chem. 257*, 10023−10029.
7. Rosevear, P. R., Chari, R. B., Kozarich, J. W., Sellin, S., Mannervik, B., and Mildvan, A. S. (1983) *J. Biol. Chem. 258*, 6823−6826.
8. Aronsson, A.-C., Sellin, S., Tibbelin, G., and Mannervik, B. (1981) *Biochem. J. 197*, 67−75.
9. Sellin, S., and Mannervik, B. (1984) *J. Biol. Chem. 259*, 11426−11429.
10. Cameron, A. D., Olin, B., Ridderström, M., Mannervik, B., and Jones, T. A. (1997) *EMBO J. 16*, 3386−3395.
11. Ridderström, M., Cameron, A. D., Jones, T. A., and Mannervik, B. (1998) *J. Biol. Chem. 273*, 21623−21628.
12. Thornalley, P. J. (1993) *Mol. Aspects Med. 14*, 287−371.
13. Murthy, N. S., Bakeris, T., Kavarana, M. J., Hamilton, D. S., Lan, Y., and Creighton, D. J. (1994) *J. Med. Chem. 37*, 2161−2166.
14. Bush, P. E., and Norton, S. J. (1985) *J. Med. Chem. 28*, 828−830.
15. Ridderström, M., and Mannervik, B. (1996) *Biochem. J. 314*, 463−467.
16. Otwinowski, Z., and Minor, W. (1997) *Methods Enzymol. 276*, 307−326.
17. Collaborative Computation Project Number 4 (1994) *Acta Crystallogr. D50*, 760−763.
18. Brünger, A. T. (1992) *Nature 355*, 472−475.
19. Brünger, A. T., Karplus, M., and Petsko, G. A. (1989) *Acta Crystallogr. A45*, 50−61.
20. Brünger, A. T. (1992) *X-PLOR version 3.1: A system for crystallography and NMR*, Yale University Press, New Haven, CT.
21. Brünger, A. T., and Krukowski, A. (1990) *Acta Crystallogr. A46*, 585−593.
22. Jones, T. A., and Kjeldgaard, M. O. (1997) *Methods Enzymol. 277*, 173−208.
23. Kleywegt, G. J., and Jones, T. A. (1994) in *From First Map to Final Model* (Bailey, S., Hubbard, R., and Waller, D., Eds.) pp 59−66, SERC Daresbury Laboratory, Daresbury, Warrington, U.K.
24. Murshodov, G. N., Vagin, A. A., and Dodson, E. J. (1997) *Acta Crystallogr. D53*, 240−255.
25. Leslie, A. G. W. (1992) Joint CCP4 and ESF-EACMB Newsletter on Protein Crystallography No. 26, SERC Daresbury Laboratory, Daresbury, Warrington, U.K.
26. Navaza, J. (1994) *Acta Crystallogr. A50*, 157−163.
27. Brünger, A. T., Adams, P. D., Clore, G. M., DeLano, W. L., Gros, P., Grosse-Kunstleve, R. W., Jiang, J.-S., Kuszewski, J., Nilges, M., Pannu, N. S., Read, R. J., Rice, L. M., Simonson, T., and Warren, G. L. (1998) *Acta Crystallogr. D54*, 905−921.
28. Rice, L. M., and Brünger, A. T. (1994) *Proteins 19*, 277−290.
29. Lamzin, V. S., and Wilson, K. S. (1993) *Acta Crystallogr. D49*, 129−147.
30. Vince, R., and Wadd, W. B. (1969) *Biochem. Biophys. Res. Commun. 34*, 593−598.
31. Vince, R., Daluge, S., and Wadd, W. B. (1971) *J. Med. Chem. 14*, 402−404.
32. Vince, R., and Daluge, S. (1971) *J. Med. Chem. 14*, 35−37.
33. Hamilton, D. S., and Creighton, D. J. (1992) *J. Biol. Chem. 267*, 24933−24936.
34. Lan, Y., Lu, T., Lovett, P. S., and Creighton, D. J. (1995) *J. Biol. Chem. 270*, 12957−12960.
35. Ridderström, M., Cameron, A. D., Jones, T. A., and Mannervik, B. (1997) *Biochem. J. 328*, 231−235.
36. D'Silva, C. (1986) *FEBS Lett. 202*, 240−244.
37. Garcia-Iniguez, L., Powers, L., Chance, B., Sellin, S., Mannervik, B., and Mildvan, A. S. (1984) *Biochemistry 23*, 685−689.
38. Sellin, S., Eriksson, L. E. G., Aronsson, A.-C., and Mannervik, B. (1983) *J. Biol. Chem. 258*, 2091−2093.
39. Sellin, S., Eriksson, L. E. G., and Mannervik, B. (1987) *Biochemistry 26*, 6779−6784.
40. Christianson, D. W. (1991) *Adv. Protein Chem. 42*, 281−355.
41. Alberts, I. L., Nadassy, K., and Wodak, S. J. (1998) *Protein Sci. 7*, 1700−1716.
42. Rosevear, P. R., Sellin, S., Mannervik, B., Kuntz, I. D., and Mildvan, A. S. (1984) *J. Biol. Chem. 259*, 11436−11447.
43. Ekwall, K., and Mannervik, B. (1973) *Biochim. Biophys. Acta 297*, 297−299.

44. Griffis, C. E., Ong, L. H., Buettner, L., and Creighton, D. J. (1983) *Biochemistry 22*, 2945−2951.
45. Rae, C., Berners-Price, S. J., Bulliman, B. T., and Kuchel, P. W. (1990) *Eur. J. Biochem. 193*, 83−90.
46. Rae, C., O'Donoghue, S. I., Bubb, W. A., and Kuchel, P. W. (1994) *Biochemistry 33*, 3548−3559.
47. Landro, J. A., Brush, E. J., and Kozarich, J. W. (1992) *Biochemistry 31*, 6069−6077.
48. Hamilton, D. S., and Creighton, D. J. (1992) *Biochim. Biophys. Acta 1159*, 303−308.
49. Engh, R. A., and Huber, R. (1992) *Acta Crystallogr. A47*, 392−400.
50. Kleywegt, G. J., and Jones, T. A. (1996) *Structure 4*, 1395−1400.

BI990696C